New Journal of Physics
The open access journal at the forefront of physics

Deutsche Physikalische Gesellschaft DPG
IOP Institute of Physics

Published in partnership with: Deutsche Physikalische Gesellschaft and the Institute of Physics

OPEN ACCESS

RECEIVED
13 May 2015

REVISED
22 September 2015

ACCEPTED FOR PUBLICATION
20 October 2015

PUBLISHED
10 November 2015

PAPER

Transport of quantum excitations coupled to spatially extended nonlinear many-body systems

Stefano Iubini[1,5], **Octavi Boada**[2], **Yasser Omar**[2,3] **and Francesco Piazza**[1,4]

[1] Centre de Biophysique Moléculaire, (CBM), CNRS-UPR 4301, Rue C. Sadron, F-45071, Orléans, France
[2] Physics of Information Group, Instituto de Telecomunicações, Lisbon, Portugal
[3] CEMAPRE, ISEG, Universidade de Lisboa, Portugal
[4] Université d'Orléans, Château de la Source, F-45071 Orléans Cedex, France
[5] Author to whom any correspondence should be addressed.

E-mail: stefano.iubini@cnrs-orleans.fr, oboada@lx.it.pt, yasser.omar@lx.it.pt and Francesco.Piazza@cnrs-orleans.fr

Keywords: exciton transport, nonlinear dynamics, noise in quantum systems

Abstract

The role of noise in the transport properties of quantum excitations is a topic of great importance in many fields, from organic semiconductors for technological applications to light-harvesting complexes in photosynthesis. In this paper we study a semi-classical model where a tight-binding Hamiltonian is fully coupled to an underlying spatially extended nonlinear chain of atoms. We show that the transport properties of a quantum excitation are subtly modulated by (i) the specific type (local versus non-local) of exciton–phonon coupling and by (ii) nonlinear effects of the underlying lattice. We report a non-monotonic dependence of the exciton diffusion coefficient on temperature, in agreement with earlier predictions, as a direct consequence of the lattice-induced fluctuations in the hopping rates due to long-wavelength vibrational modes. A standard measure of transport efficiency confirms that both nonlinearity in the underlying lattice and off-diagonal exciton–phonon coupling promote transport efficiency at high temperatures, preventing the Zeno-like quench observed in other models lacking an explicit noise-providing dynamical system.

1. Introduction

Transport of quantum excitations in complex low-dimensional systems is a topic of paramount importance in many physical contexts, such as semiconductor nanowires and nanotubes [1], metallic wires [2], ultracold atom systems in one-dimensional optical lattices [3], quasi one-dimensional organic superconductors, such as semiconducting [4] and metal carbon nanotubes [5], π-conjugated polymers [6] and more complex quasi-1D nano-architectures for modern technological applications [7], including plastic light-emitting devices and organic solar cells [8].

Due to their crucial role in directing light energy to reaction centers during the early stages of photosynthesis [9], excitons occupy a prominent role among the studied quantum excitations [10]. The exciton concept was introduced in solid-state physics by Frenkel in 1931 [11]. However, it was not until the 1948 seminal paper by Davydov [12] that this idea was applied to geometry-determined molecular systems, such as molecular crystals. These and related studies have paved the way for the investigation of exciton transport in light-harvesting biomolecules, which contain embedded networks of light-absorbing pigments [10].

Considerable boost to the investigation of exciton transport in biomolecules has been brought about by recent advances in 2D photon echo experiments, which have revealed unusually long decoherence times for excitons in light-harvesting complexes [13–16] and conjugated polymer systems [17]. Moreover, theoretical evidence has been accumulated that noise in certain regimes could act as a *protective* factor for quantum coherences [18–20], increasing suitably defined measures of quantum efficiency related to the transfer of electronic excitation energy from a chromophore to a distant one. In turn, such findings have corroborated more detailed investigations of the coupled dynamics of exciton transfer and protein vibrations, pointing at a

functional role of specific vibrational modes in promoting possibly function-related, long-lived electronic coherences [21–28].

However, despite the great experimental and theoretical advances, many fundamental questions remain open. In particular, pinpointing the *structural* determinants of the electron–phonon coupling that seem to provide noise-induced protection of exciton dephasing remains a challenging task. Moreover, few studies have addressed the role of the *dynamical* determinants of such mechanisms, i.e. the influence of specific inter-atomic and inter-molecular potential energy terms beyond the harmonic approximation. Importantly, nonlinearity is known to play a subtle role in many quantum transport processes, from heat conduction [29] and vibrational energy transfer [30–32] to photon-assisted electronic transport in different nanostructures [33]. More generally, it is well known that nonlinear effects modulate non-trivially transport in disordered dynamical systems [34–38].

Another issue of paramount importance that needs further investigation concerns the details of how the environment (e.g. the degrees of freedom of the protein in photosynthetic complexes) couples to the quantum degrees of freedom. In a tight-binding (TB) perspective, where the quantum excitation is characterized by a given set of site energies $\{\epsilon_i\}$ and hopping rates $\{\mathcal{J}_i\}$, this means investigating the effects of the specific functional dependence of $\{\epsilon_i, \mathcal{J}_i\}$ on the degrees of freedom of the environment (*dynamical* disorder). For example, letting only site energies fluctuate with the environment amounts to adding a pure dephasing term to the unitary evolution in the Liouville equation for the time evolution of the one-particle density matrix of the quantum excitation. It has been proved that this leads to noise-enhanced transfer efficiency [19, 20]. However, it has been observed that pure dephasing is not a physically realistic scheme of coupling and that in general fluctuations of the hopping rates, even if smaller than those of the site energies, can have a considerable impact on the dynamics of quantum excitations [39, 40]. For example, this is the case of high-mobility organic crystals, such as pentacene and rubrene, where large fluctuations in the hopping rates occur at room temperature [41, 42]. In this case, it has been shown that Zeno effect at high dephasing rates is suppressed and one recovers asymptotic mobility of the quantum excitation at increasing noise, albeit with a diffusion coefficient that decreases with temperature [43–45].

Motivated by the above described open questions, in this paper we adopt a semi-classical modeling strategy to investigate the effect of noise on the mobility and transfer efficiency of a quantum excitation coupled to the vibrations of a one-dimensional atomic chain. More specifically, the two main points that we wish to address are: (i) the role of nonlinearity of the interatomic potentials of the underlying lattice and (ii) the role of local versus non-local dynamical disorder.

The structure of this paper is as follows. In section 2 we briefly discuss existing modeling strategies and present the microscopic model that we study in this paper, describing a quantum-mechanical quasiparticle (e.g. an exciton or an electron) hopping on a one-dimensional lattice [6]. In section 3 we present the main results regarding the spreading properties of an initially localized state in a thermalized one-dimensional chain. In section 4 we analyze the quantum transport efficiency in our model in the presence of finite local recombination rates. Finally, in section 5 we summarize our conclusions and further discuss our main results.

2. Exciton-lattice coupled dynamics

The time evolution of non-isolated (open) quantum systems, i.e. systems in contact with a thermal bath, is an extremely difficult problem in general [46, 47]. Several approximate schemes have been proposed, including master equation approaches [44, 48–50] usually based on the projection operator technique [51], different non-perturbative methods [52–54] and path-integral based methods [55–57]. In some cases the exact solution of the master equation can be determined analytically [58].

Other molecular modeling approaches allow to consider a greater amount of microscopic detail through ab-initio simulations of both the quantum and the bath (e.g. the protein) degrees of freedom. These techniques combine molecular dynamics simulations for the dynamics of the environment with the time integration of the Schrödinger equation for the reduced quantum system, based on quantum electronic structure calculations [23, 59–62]. Such methods, often referred to as quantum mechanics/molecular mechanics are more sophisticated and detailed modeling schemes belonging to a more general family of modeling strategies, where the full quantum evolution of the system is parametrized by the classical coordinates of the underlying lattice/protein, that evolves in parallel according to Newton equations. Such schemes have been applied with success to a variety of problems, including energy and charge transport in polypeptide chains [63] and other biomolecules [31, 64–66].

[6] Without loss of generality, we will refer to the quantum quasiparticle in the following as the *exciton*.

In the TB approximation, the most general Hamiltonian governing the propagation of an exciton coupled to a one-dimensional lattice can be written as

$$H = \sum_{nm} J_{nm}\left(u_n, u_m\right)B_n^{\dagger}B_m + \sum_m \frac{p_n^2}{2M} + \sum_{mn} V\left(u_n, u_m\right), \tag{1}$$

where M is the bead mass, $B_n^{\dagger}$ is an exciton creation operator at site n, and u_n is the displacement of the nth mass with respect to its equilibrium position. The term $V(u_n, u_m)$ represents the total potential energy of the nodes m and n including possible onsite terms The energies $J_{nm}(u_n, u_m)$ describe the modulation of the quantum Hamiltonian due to the fluctuations of the underlying chain. In principle, depending on the physical nature of the system, both the site energies ($n = m$ terms) and the hopping rates ($n \neq m$ terms) can be be influenced by the vibrations of the chain atoms.

The Hamiltonian in equation (1) describes a general class of semi-classical models, including the Davydov [67, 68], the Holstein [69, 70], and the Su–Schrieffer-Heeger [71] Hamiltonians, that have been employed to describe the dynamics of different kinds of quantum excitations in a variety of physical systems. In such modeling schemes, one treats the exciton as a quantum mechanical particle, while describing the oscillations of the lattice classically. Thus, the equations of motion (EOM) are given by a time-dependent effective Hamiltonian for the exciton, which depends on the lattice variables u_n. The EOMs for the chain are those of a set of coupled oscillators driven by the exciton wave function.

In this paper we specialize to a nearest-neighbor TB scheme with fully fluctuating parameters (i.e. both site energies and hopping rates), coupled to a nonlinear Fermi–Pasta–Ulam (FPU) chain [72]. The FPU potential can be derived as a fourth-order Taylor expansion of a generic nearest-neighbor interaction potential with respect to the equilibrium positions of the chain. For the sake of simplicity we will neglect cubic terms, which are known to give rise to specific topological (kink) excitations in the system, where also the equilibrium position of atoms are shifted and also to more complex combined breather-kink modes [73].

The Hamiltonian governing the system is the sum of two terms $H = H_{\mathrm{e}} + H_{\mathrm{l}}$. H_{e} is the Hamiltonian for an exciton propagating on the lattice in a given dynamical configuration, while H_l is the lattice Hamiltonian. Explicitly, we have

$$H_{\mathrm{e}} = \sum_{n=1}^{L}\epsilon_n(u)B_n^{\dagger}B_n + \sum_{n=1}^{L}J_n(u)\left(B_{n+1}^{\dagger}B_n + B_n^{\dagger}B_{n+1}\right) \tag{2}$$

and

$$H_{\mathrm{l}} = \sum_{n=1}^{L}\left[\frac{p_n^2}{2M} + \frac{\kappa}{2}\left(u_{n+1} - u_n\right)^2 + \frac{\beta}{4}\left(u_{n+1} - u_n\right)^4\right], \tag{3}$$

where L is the lattice size, M is the mass of the atoms and β is the anharmonicity parameter. The operator B_n ($B_n^{\dagger}$) destroys (creates) an exciton at the position occupied by the nth bead.

According to our scheme, the energies appearing in the exciton hamiltonian H_{e} are renormalized over time by the lattice fluctuations, namely

$$\epsilon_n = E_n^0 + \chi_E\left(u_{n+1} - u_{n-1}\right), \tag{4}$$

and

$$J_n = J_n^0 + \chi_J\left(u_{n+1} - u_n\right). \tag{5}$$

In the above equations, the 0 superscript refers to the unperturbed values of site energies and hopping integrals, while the parameters χ_E and χ_J gauge the strength of the exciton-lattice coupling. In the following we will consider $E_n^0 = J_n^0 = 1 \forall\ n$, unless specifically stated otherwise. Notice that with the above choice of coupling the total Hamiltonian is invariant under global spatial translations of the u_n, so that the total momentum of the lattice is conserved during the evolution. Moreover, the invariance of the Hamiltonian under phase transformations of the variables B_n guarantees the conservation of the total excitonic probability. Equations (4) and (5) are a natural way to minimally couple the exciton to the chain, as they can be seen as the first order term of a Taylor expansion of the effective local energies and exchange integrals in powers of u_n.

In our semi-classical approach, only the exciton state is treated quantum-mechanically, while the lattice variables u_n evolve according to the laws of classical mechanics. As we work in the single-exciton manifold, in order to determine the time-evolution of the system we consider a trial wave-function for the exciton in the form

$$|\psi(t)\rangle = \sum_n b_n^*(t)\ B_n^{\dagger}\ |0\rangle \tag{6}$$

and derive the appropriate coupled EOMs for the coefficients b_n and lattice variables u_n. The amplitudes b_n^* define the wavefunction in the basis of lattice sites. In the following we will always impose the normalization

condition $\sum_n |b_n|^2 = 1$. The time evolution of the coefficients b_n follows directly from Schrödinger's equation

$$\mathrm{i}\hbar\frac{\mathrm{d}b_n}{\mathrm{d}t} = -\epsilon_n b_n, -J_n\left(b_{n+1} + b_{n-1}\right), \tag{7}$$

where the parameters J_n and ϵ_n are those of equations (4) and (5), and depend on the lattice variables. The EOMs of the underlying lattice are obtained from the expectation value of the Hamiltonian on the exciton wavefunction, that is

$$\begin{aligned} M\ddot{u}_n &= -\frac{\partial}{\partial u_n}\langle\psi|\ H\ |\psi\rangle \\ &= F_n^l + F_n^e \end{aligned} \tag{8}$$

with

$$\begin{aligned} F_n^l &= \kappa\left(u_{n+1} + u_{n-1} - 2u_n\right) + \beta\left[\left(u_{n+1} - u_n\right)^3 + \left(u_{n-1} - u_n\right)^3\right] \\ F_n^e &= \chi_J\left(b_{n+1}^* b_n + b_{n-1}^* b_n\right) + \chi_E\left(b_{n+1}^* b_{n+1} + b_{n-1}^* b_{n-1}\right). \end{aligned} \tag{9}$$

In the following we will take $\kappa = M = 1$ so that the upper frequency of the linear spectrum of the chain is $\omega_0 = \sqrt{2}$. Moreover, throughout this paper we consider periodic boundary conditions. It is worth noting that equations (7) and (8) also correspond to the deterministic version of a set of equations that can be derived through a path-integral approach [55]. Furthermore, we observe that, despite our choice of a bilinear exciton-lattice coupling, the ensuing time evolution governed by equations (7) and (8) is a nonlinear one.

For the analysis reported in the following, we evolved numerically the coupled EOMs (7) and (8) starting from different initial conditions and referring both to equilibrium and non-equilibrium setups. For this we used a standard 4th order Runge–Kutta algorithm with a time step $\mathrm{d}t = 10^{-3}$. In particular, we prepared the lattice initial condition by sampling a characteristic configuration of the variables u_n and p_n representative of a finite temperature T. This task is accomplished by thermalizing the lattice via a Langevin heat bath [74] at temperature T for a sufficiently long transient time t_0. Explicitly, the Langevin thermalization is achieved by augmenting the free lattice EOMs with a suitable friction term and a stochastic force, namely

$$\ddot{u}_n = F_n^l - \alpha p_n + \sqrt{2\alpha T}\,\xi_n(t), \tag{10}$$

where α defines the coupling strength of the reservoir and $\xi_n(t)$ is a Gaussian white noise with zero mean and unit variance. Notice that the present setup corresponds to the thermalization of each site of the lattice chain with an independent heat bath at temperature T (measured setting the Boltzmann constant $k_\mathrm{B} = 1$). Moreover, for all the simulations we will set $t_0 = L$ and $\alpha = 1$. This choice of parameters guarantees an efficient thermalization of the lattice in the whole range of parameters studied in this paper. Finally, once the lattice has reached a stationary, thermalized state, the Langevin reservoir is disconnected in order to sample the microcanonical dynamics of the total (lattice + exciton) system.

2.1. Equilibrium spectral analysis

The explicit treatment of the lattice dynamics by means of equation (8) represents a simple and direct way to include more realistic, *explicit* spatio-temporal correlations in the environmental noise that perturbs the exciton evolution, as opposed to more abstract treatments where the environment only enters the picture as a *spectral density*. It is therefore interesting to provide a spectral characterization of the lattice dynamics, focusing on equilibrium stationary states at a given temperature T. The same analysis also allows us to explore the near-equilibrium exciton transfer processes.

In order to show the relevant transport properties of the lattice, it is instructive to look at the power spectra of its long-wavelength Fourier modes. These are reported in the upper panel of figure 1. Simulations have been performed evolving the system in the presence of a Langevin thermal bath at temperature T [74] for a transient time $t_0 = L$. We remark that, according to our prescriptions, time in our simulations is measured in units of $\sqrt{M/\kappa}$. The external heat bath was switched off at $t = t_0$ and the power spectrum was then computed by sampling the microcanonical dynamics over an interval of 2^{16} temporal units and averaging over different thermalized initial conditions.

For a white-noise signal, one would obviously observe a flat spectrum. The sharp peaks that are visible in figure 1 flag the nontrivial propagation of correlations inside the nonlinear chain. Their presence is also closely related to the anomalous heat transport properties observed in the FPU chain [74] and clearly shows that the lattice dynamics cannot be approximated by a diffusive uncorrelated process like a pure-dephasing (PD) noise. We conclude that nonlinearity in the interatomic potentials of the underlying dynamical system couples the exciton to a noise possessing a complex structure. This is likely to be the case *a fortiori* for excitons propagating

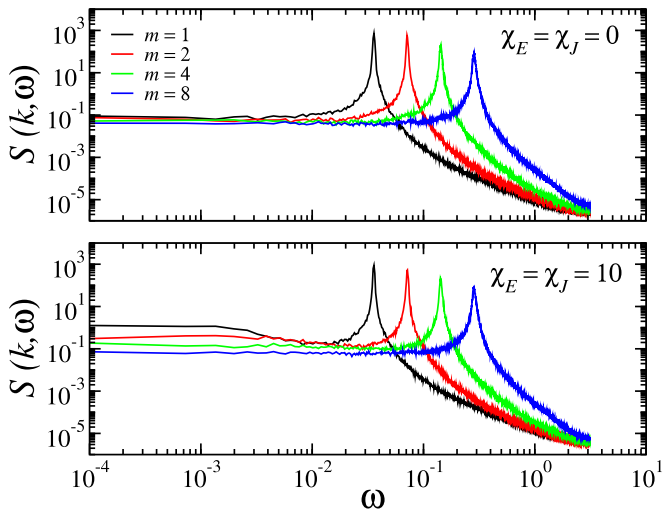

Figure 1. Equilibrium power spectra $S(k, \omega)$ of the lattice dynamics (power spectrum of the time series $\sum_n u_n(t)\mathrm{e}^{\mathrm{i}kn}$) for low-$k$ Fourier modes with $k = 2\pi m/L$ and $m = \{1, 2, 4, 8\}$ for a thermalized nonlinear chain with $T = 1, \beta = 1$ and $L = 256$. The upper panel refers to an isolated lattice, while the lower panel shows the lattice spectrum in a regime of a strong coupling with the exciton. Each spectrum is computed by averaging over 50 independent realizations of the dynamics.

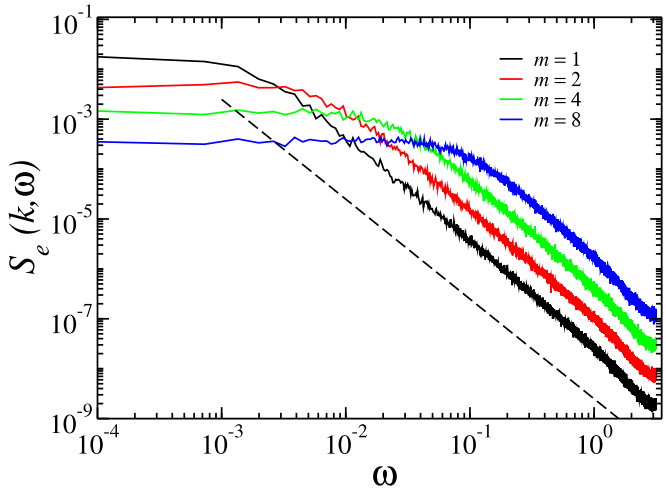

Figure 2. Power spectra $S_e(k, \omega)$ of the exciton amplitudes (i.e. power spectra of the time series $\sum_n |b_n(t)|^2 \mathrm{e}^{\mathrm{i}kn}$) for an exciton-lattice coupling $\chi_E = \chi_J = 1$ in a chain with $T = 1, \beta = 1$ and $L = 256$ (with $k = 2\pi m/L$). Each spectrum is computed by averaging over 50 independent realizations of the dynamics of the underlying lattice. The dashed black line is a power-law with exponent -2 and indicates the characteristic diffusive behavior.

within complex fluctuating biomolecules. The necessity of including the proper correlations in the noise beyond PD, possibly encoded in the underlying lattice structure, appears therefore important.

We then move on to examine the lattice spectrum in the presence of non-vanishing exciton-lattice coupling, as this can inform on the back-action exerted by the exciton on the underlying dynamical system. In this situation, the thermalization process and the following free dynamics were performed by evolving the coupled equations (7) and (8) with an excitonic initial condition corresponding to a random-phase delocalized state. The corresponding lattice spectra are shown in the lower panel of figure 1. We find that, even in the regime of strong coupling, the relevant features of the characteristic peaks are essentially unchanged. The only difference with the zero-coupling case is a slight deformation of the low-frequency and low-wavenumber region of the spectrum. We therefore conclude that our combined exciton-lattice model exhibits environmental correlations that generally survive for finite temperatures and coupling strengths.

It is instructive to carry out a similar spectral analysis also for the excitonic degrees of freedom. In figure 2 we show the power spectrum $S_e(k, \omega)$ of the exciton amplitude field $|b_n(t)|^2$ in the presence of a thermal background at finite temperature. The spectrum of each normal mode k is well fitted by a Lorentzian distribution, a manifest

evidence that sufficiently strong perturbations resulting from the underlying lattice dynamics produce a diffusion-dominated exciton transport.

It is important to observe that the spectral analysis reported here allows to explore the out-of-equilibrium properties of the exciton-lattice chain only perturbatively, i.e. in the spirit of linear-response theory. On the other hand, many realistic situations are characterized by strong out-of-equilibrium conditions. For example, this is the case of the propagation of photosynthetic excitons created in light-harvesting antenna complexes following the absorption of a photon. Such physical scenarios properly correspond to far-from-equilibrium initial condition that cannot be included in linear-response schemes. For this reason, in the next section we discuss in detail non-stationary exciton transport arising from spatially localized initial conditions.

3. Exciton spreading on a chain at finite temperature

In this section we study the spreading of an initially localized exciton wave-function interacting with the chain. The initial conditions for the lattice are taken by sampling random velocities from a Maxwell distribution at a given temperature T, which is one of the parameters in these simulations. The initial displacements are set to zero. The lattice is then evolved for a transient time $t_0 = L$ in the presence of a Langevin heat bath at temperature T that interacts independently with each site of the chain [74]. After this thermalization process, the external heat bath is disconnected and the lattice-exciton interaction term in the Hamiltonian is switched on. Furthermore, we average the time evolution of the same initial condition for the exciton over many independent trajectories, each corresponding to different initial conditions of the chain sampled from the same thermal distribution. In our picture, the decoherence of the exciton wave-function is brought about by averaging over many independent realizations of the explicit noise (the lattice dynamics).

For sufficiently low temperatures and couplings, one can argue that the exciton evolution should be only weakly perturbed by the environment. Indeed, the exciton is found to spread over the chain almost ballistically in this regime, with a slow loss of coherence. However, one may speculate that for larger values of couplings and temperatures the non-Markovian nature of the noise acting upon the exciton and the nonlinearity of the dynamics may play a fundamental role in modulating the spreading of an exciton. For instance, very large couplings typically result in the emergence of immobile self-trapped states of nonlinear origin. The net effect is that a substantial amount of the vibrational energy gets pinned around a handful of sites in the chain, producing a pinning potential where the exciton self-traps, making *de facto* impossible any kind of exciton transport. Self-trapped states are well-known in many problems studied with models belonging to the same class as ours, such as the Holstein polaron [69, 70] and discrete breathers (DBs) in dilute Bose–Einstein condensates trapped in optical potentials [75–78].

The situation is perhaps more interesting at intermediate couplings, where it is not clear *a priori* over what timescale the spreading is diffusive and what is the dependence of the exciton diffusion constant D on the lattice temperature.

In order to gather information on the fraction of lattice sites that are significantly occupied during the time evolution of the system, we compute the participation ratio Π, defined as

$$\Pi(t) = \frac{\sum_n \left|b_n(t)\right|^2}{\sum_n \left|b_n(t)\right|^4} - 1 = \frac{1}{\sum_n \left|b_n(t)\right|^4} - 1. \tag{11}$$

With this choice of normalization, it is easy to show that $\Pi = 0$ for a completely localized exciton wavefunction, while one has $\Pi = L$–1 for a perfectly uniform state. Therefore, one should think at Π as an effective *length*, measuring the spatial extent of the exciton wavefunction over the chain. As such, diffusive spreading would be flagged by a law of the type $\Pi(t) \propto t^{1/2}$, while ballistic propagation would correspond to a linear dependence on time, $\Pi(t) \propto t$.

In figure 3 we show the typical time evolution of the participation ratio for different coupling strengths and $T = 0.1$. The first stage is a short transient ($t \lesssim 1$), where Π grows quadratically in time. This *super-ballistic* evolution is characteristic of the very first stage of the time evolution of an initially localized wavefunction. This can be easily proved by writing down equations (7) for an exciton initially sitting entirely at site n in a chain with $J_n = J \forall\ n$. In this case it is not difficult to show that, if one defines $Q(t) = |b_n(t)|^2 - |b_{n\pm1}(t)|^2$ (with $Q(0) = 1$), then

$$Q(t) = \exp\left[-\frac{1}{\tau^2}\int_0^t \sin 2\Delta\phi\ \Delta\dot{\phi}^{-1}\,\mathrm{d}t'\right], \tag{12}$$

where $\tau = \hbar/(2J)$ and $\Delta\phi = \phi_{n\pm1} - \phi_n$ is the phase difference between the initially excited site and its neighbors. Without loss of generality, in the spirit of a Taylor expansion, we can assume $\Delta\phi \simeq t/\tau$ in the early

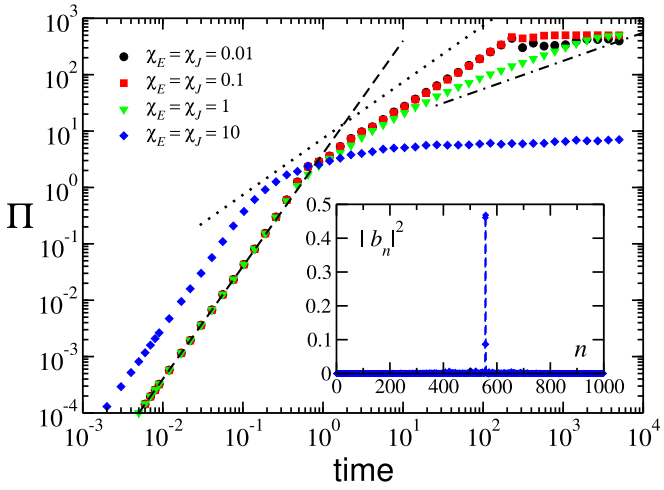

Figure 3. Evolution of $\Pi(t)$ for $T = 0.1$ and different couplings in a chain with $L = 1000$ lattice sites. The dashed line is a plot of the initial super-ballistic propagation $\Pi(t) = (t/\tau)^2$ with $\tau = \hbar/(2J)$. Dotted and dotted–dashed lines indicate a power-law growth of the kind t^α with $\alpha = 1$ (ballistic) and 0.5 (diffusive), respectively. The inset shows the final profile of $|b_n|^2$ for the largest coupling $\chi_E = \chi_J = 10$. A self-trapped state is clearly observable around the center of the chain.

stages of the propagation. It is then straightforward to show that this immediately leads to a super-ballistic trend, namely $\Pi(t) \simeq (t/\tau)^2$. It is apparent from figure 3 that this prediction is in excellent agreement with the simulations for low and moderate couplings. For larger values of the coupling, the physical law does not appear to change, while the time constant turns out to be renormalized. For example, for $\chi_E = \chi_J = 10$ we get $\Pi(t) \simeq (t/\tau')^2$ with $\tau' = \tau/3$, which means faster super-ballistic propagation for large coupling strengths. It is intriguing to observe that this first super-ballistic stage could be physically relevant in many contexts. For example, in light-harvesting complexes one typically has $J \simeq 100$ cm^{-1}, i.e. $\tau \simeq 170$ fs, which is of the same order of magnitude as the observed lifetime of quantum beats in 2D photon echo spectroscopy at room temperature [13].

In the subsequent evolution for times greater than $\tau = \hbar/(2J)$, we can single out two main regimes corresponding to different dynamical situations. At low couplings, we recover the expected almost unperturbed evolution associated with ballistic spreading of the exciton, i.e. $\Pi(t) \propto t$. The plateau observed at long times in figure 3 for $\chi_E = \chi_J = 0.01$ and 0.1 simply signals that the exciton wavefunction has reached complete delocalization (the lattice is finite) and no further spreading is thus possible. For intermediate couplings, it is clearly possible to observe a transition from a ballistic to a diffusive ($\Pi(t) \propto t^{1/2}$) regime. Overall, we conclude that for intermediate couplings one should always expect a ballistic-to-diffusive crossover, the time scale associated with it decreasing with increasing coupling.

The situation changes rather dramatically for large values of the coupling strengths. In this case, the system enters a strongly nonlinear regime, where the localized initial condition triggers the spontaneous creation of a stable self-trapped state of nonlinear origin, which results in a very slow sub-diffusive transport (see also the inset of figure 3). Increasing the coupling further causes the initial amplitude of the exciton to stay permanently stored in a localized, time-periodic excitation of the system which is virtually decoupled from the rest of the system (see [77] for a comprehensive review on DBs in nonlinear lattices). It is important to point out that the asymptotic stability of the self-trapped state depends both on the strength of the coupling $\chi_E = \chi_J$ and on the temperature T. In particular, for certain critical values χ_c and T_c, such localized structures become unstable and get quickly destroyed by the thermal fluctuations of the lattice [79, 80]. On the other hand, the ballistic and diffusive regimes shown in figure 3 are not separated by a true dynamical transition. In fact, one can argue that for sufficiently long chains and times, any arbitrarily small interaction with the lattice will eventually cause a diffusion of the excitonic wavepacket.

For the exciton nonequilibrium evolution reported in figure 3 we have also monitored the lattice kinetic temperature T_k *measured* after the Langevin heat bath has been disconnected. T_k is defined as

$$T_k(t) = \frac{1}{L}\sum_{n=1}^{L}\left[\left\langle p_n^2(t)\right\rangle - \left\langle p_n(t)\right\rangle^2\right], \tag{13}$$

where the symbol $\langle\cdot\rangle$ refers to a classical average over the set of independent lattice trajectories. Figure 4 illustrates the evolution of T_k for the same setup of figure 3, which corresponds to a temperature of the Langevin bath $T = 0.1$. Interestingly, in a wide region of coupling values that keep the overall system out of the strongly nonlinear regime, T_k remains close to the Langevin temperature during the whole exciton evolution. Conversely, the emergence of a stable discrete breather for large coupling strengths, $\chi_E = \chi_J = 10$ (see blue diamonds of

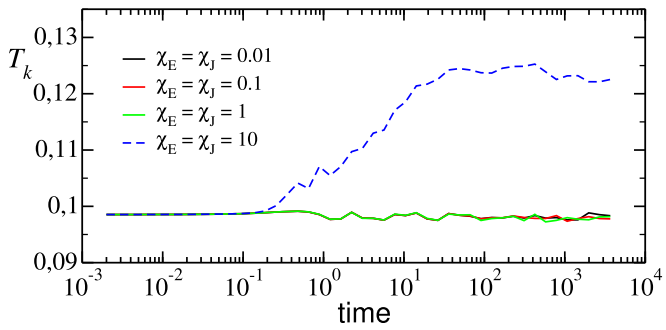

Figure 4. Evolution of the lattice temperature T_k (see equation (13)) during the exciton spreading dynamics shown in figure 3.

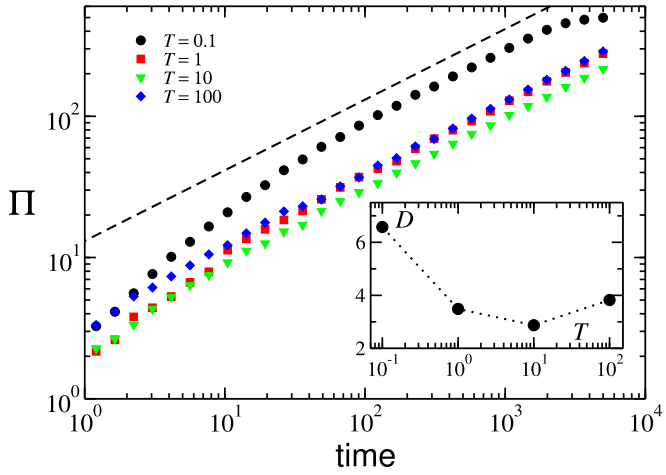

Figure 5. Time evolution of $\Pi(t)$ for $\chi_E = \chi_J = 1$ and different temperatures of the lattice. The inset shows the behavior of the diffusion constant measured by fitting a power law to the asymptotic portion of the spreading. The dashed line is a plot of a power law with exponent 1/2.

figure 3), produces a clear increase of T_k, which is associated with the conversion of a substantial portion of lattice energy into (negative) exciton-lattice interaction energy. Accordingly, by virtue of the conservation of the total energy of the system, such energy transfer causes the lattice to heat up. However, this should be regarded as a finite-size effect. In general, we expect that, upon increasing the lattice length L, the heating effect becomes less and less important until it should eventually disappear in the thermodynamic limit $L \to \infty$, since the breather interaction energy is localized over a finite number of lattice sites, whereas the lattice energy scales linearly with L. Altogether, the above analysis confirms the consistency of the lattice dynamics as a well defined *explicit* thermal environment.

3.1. The effective diffusion constant

From the above discussion it is clear that in the intermediate coupling regime the asymptotic dynamics is diffusive. We now turn to analyzing in detail the properties of the diffusive spreading by a characterization of the diffusion constant D, defined as

$$D = \lim_{t\to\infty} t^{-1/2}\Pi(t). \tag{14}$$

In figure 5 we compare the growth of $\Pi(t)$ for increasing temperatures T and fixed values of the couplings $\chi_E = \chi_J = 1$ in the intermediate regime. Interestingly, we find a nonmonotonic behavior for the dependence of the diffusion constant on the temperature T. More precisely, we observe a minimum located around $T = 10$, indicating the presence of a slowed-down spreading dynamics at intermediate temperatures.

This phenomenon can be illustrated more effectively by measuring the average time t_s it takes for the participation ratio to reach a certain threshold value Π_s. In this *temporal representation* a minimum in the diffusion constant D corresponds to a maximum of the time t_s. The value of Π_s needs to be chosen in such a way as to avoid both the transient dynamics (typical of short times) and the saturation of $\Pi(t)$ due to the finite size of the considered lattices (see again figure 5). Accordingly, we have chosen $\Pi_s = 100$ for a chain of $L = 1000$ sites.

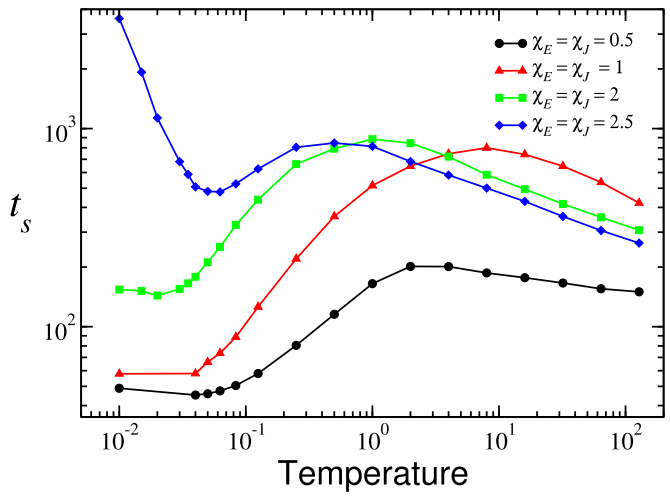

Figure 6. The average time t_s needed to attain a participation ratio $\Pi_s = 100$ as a function of temperature T for different values of the coupling strengths. The chain length is $L = 1000$.

The dependence of t_s on temperature is illustrated in figure 6 for increasing couplings. For the lowest coupling considered, t_s displays an initial growing stage, followed by a decrease at high temperatures after a maximum, which becomes more and more distinguishable upon increasing the coupling (note the logarithmic scale on the y axis in figure 6). Interestingly, this maximum appears to move towards smaller and smaller temperatures at increasing coupling strengths. This feature should be compared with the data displayed in the inset in figure 5, illustrating a minimum of the transport coefficient associated with exciton transport. A stationary point at the same value of temperature $T \approx 10$ is indeed recovered in both mobility indicators, D and t_s.

The sudden growth of t_s in the low-temperature region for $\chi = 2.5$ flags the presence of self-trapped, breather-like excitations, which pin energy locally and thus slow down the relaxation process. This kind of localized states, however, are not present at the temperatures characterizing the maximum of t_s, since the strength of thermal fluctuations is too large to sustain coherent localized nonlinear vibrations [79, 80].

The above analysis suggests that the nonmonotonicity displayed by transport coefficients with temperature is not related directly to nonlinear localization phenomena that pin energy down at high temperatures. It is therefore highly likely that the observed transport behavior is directly linked to the specific way the lattice vibrations couple to the parameters entering the exciton Hamiltonian. In fact, in the limit case of spatially uncorrelated white noise, it has been long known that local and nonlocal perturbations of the coherent Schrödinger dynamics can produce dramatically different behaviors for the spreading of an initially localized excitation [43]. In particular, it is known that purely local noise (in our picture, dynamical modulation of the site energies only) results in suppression of transport for large dephasing rates (a phenomenon often considered as an instance of the quantum Zeno effect [20, 81]).

With these ideas in mind, we turned to examine the role of the effective noise acting on the free exciton dynamics as a consequence of the lattice thermal fluctuations. In the same spirit as the analysis performed in [43], we simplified the coupling between the exciton and the lattice by studying separately diagonal (involving site energies) and off-diagonal (involving hopping rates) interactions.

In figure 7 we compare the spreading diffusion constant of a system exhibiting only diagonal coupling ($\chi_J = 0$) with the one corresponding to a pure off-diagonal coupling ($\chi_E = 0$). Interestingly, the nonmonotonic behavior of D is present only in the latter case, while in the former we observe a monotonic decrease of D with temperature. This is precisely what happens in a master equation description *à la* Haken and Strobl [44] with nearest-neighbor Coulomb coupling, where

$$D = 2\gamma_1 a^2 + \frac{a^2 J^2}{\hbar^2\left(\gamma_0 + 3\gamma_1\right)}. \tag{15}$$

Here γ_0 and γ_1 are the diagonal (pure dephasing) and off-diagonal noise strengths, J is the Coulomb hopping integral and a is the lattice spacing. The results of our simulations performed with $\chi_J = 0$ are in agreement with the prediction (15) with $\gamma_1 = 0$, that is, a value of D which decreases monotonically with temperature (γ_0 in the language of [44] and [20]. In fact, the effect of purely local perturbations of the excitonic energy is to produce a diffusion of the Schrödinger phases that inhibits quantum transport. Eventually, in the limit of infinite

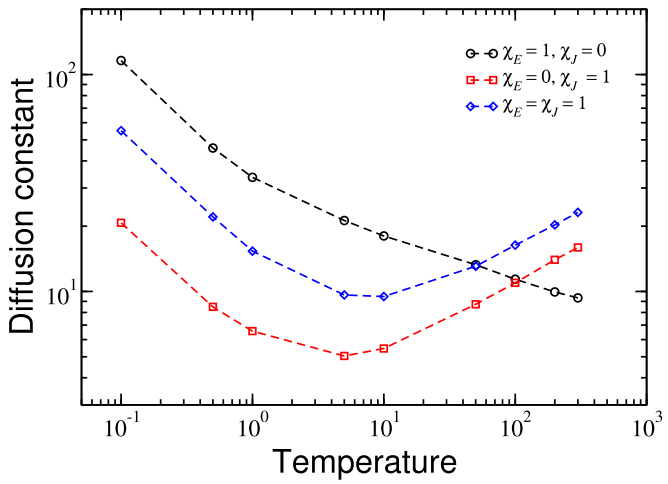

Figure 7. Temperature dependence of the spreading diffusion constants D in the presence of purely diagonal interaction (black circles) and purely off-diagonal interaction (red squares). Blue diamonds refer to the *full* model, with $\chi_E = 1$ and $\chi_J = 1$. Other parameters are $L = 1000$ and $\beta = 1$.

interaction (i.e. infinite temperature), the quantum system remains frozen in the initial condition ($D = 0$) as a consequence of the complete randomization of the phases.

The situation changes when we let the hopping rates be modulated by the lattice dynamics ($\chi_J \neq 0$, i.e. $\gamma_1 \neq 0$). As can be appreciated from figure 6, the diffusion constant displays a minimum, in agreement with the general prediction (15) and the transport becomes faster at increasing temperatures. In fact, since both phase and amplitude perturbations are now allowed for, the limit of infinite temperature corresponds to an arbitrarily large diffusion constant. This result can be interpreted as a recovery of classical amplitude diffusion in the infinite temperature limit. On more formal grounds, it can be shown that such classical reduction allows one to reduce a generalized Lindblad equation [43] for the exciton density matrix to a classical Fokker–Planck equation for the amplitude probability distribution. Although the non-Markovian nature of the effective noise and the explicit nonlinearity make the analytical calculation of $D(T, \chi_E, \chi_J)$ extremely difficult, the numerical results reported in figure 7 clearly indicate that classical diffusion is recovered also when one considers the full model with both local and nonlocal couplings.

Interestingly, we remark that at low temperatures pure-diagonal noise allows for the fastest transport. However, as non-diagonal noise results in a minimum, the situation reverses beyond a characteristic temperature when χ_J is *switched on*. In this case, the model with fluctuating coupling strengths becomes the one affording more rapid spreading at high temperatures.

It is interesting to note that extended vibrational modes are required in order to observe a nonmonotonic behavior of the diffusion constant, signaling a nontrivial coupling between exciton spreading and *collective* modes of the underlying lattice. This can be appreciated by comparing our analysis with the results presented in [45], where the hopping rates in the TB exciton Hamiltonian are modulated by the dynamics of a set of *uncoupled* harmonic oscillators. In this case, the authors report values of the diffusion coefficient that decrease monotonically with temperature. This is possibly a consequence of the absence of coupling between the oscillators providing the noise. Alternatively, they might be just exploring the low-temperature regime, as defined by their parameters.

From figure 7 one can also argue that the effective interaction experienced by the exciton for finite temperatures can not be mapped onto a spatially and temporally uncorrelated noise as in [43]. Specifically, we find that the spreading problem for pure local exciton-lattice interactions is ruled by a nontrivial power-law decay $D(T) \sim T^{-\gamma}$ with $\gamma \approx 0.3$ (data in figure 7), whereas $\gamma = 1$ for white noise [43]. In the absence of nonlinearity in the lattice Hamiltonian ($\beta = 0$), the characteristic exponent is found to be close to $\gamma \simeq 0.6$, as shown in figure 8. We therefore identify two different sources of slowing down in the transport, that are characteristic of the explicit lattice dynamics. The first one is due to the presence of spatio-temporal correlations in the lattice system. The second one is associated with explicit nonlinear terms in the lattice pairwise potential energies $V(u_n, u_m)$.

Overall, the above detailed analysis allows us to conclude that the high-temperature limit of excitonic systems interacting with noisy environments is crucially determined by the specific properties of the exciton-lattice coupling and by the nature of the spatio-temporal correlations that characterize the noise-providing underlying lattice. In particular, the presence of non-diagonal coupling is sufficient to suppress localization at

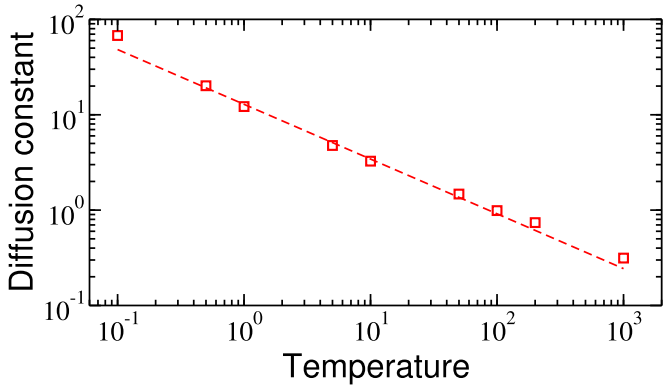

Figure 8. Temperature dependence of the spreading diffusion coefficient D for an harmonic chain ($\beta = 0$) with pure diagonal coupling ($\chi_E = 1$ and $\chi_J = 0$). The red line is a power law fit with a function $D \propto T^{-\gamma}$ with $\gamma = 0.58$.

high temperatures, which can be regarded as the semiclassical counterpart of the quantum Zeno effect observed in quantum master equation approaches [20].

An interesting consequence of the above reasoning is that the standard scenario for noise-assisted quantum transfer efficiency [19, 20] may display novel structures when passing from local pure dephasing noise to more realistic models of coupling including amplitude-affecting terms in the non-Hermitian part of the Hamiltonian. We thus turn now to discussing the implications of our explicit-noise approach for the efficiency problem.

4. Exciton energy transport efficiency

A quantum excitation such an exciton has an intrinsic lifetime, which is dictated by the recombination rate γ_r associated with the specificities of the environment. For example, in light-harvesting systems γ_r is estimated to be about 1 exciton per nanosecond [20]. The quantum excitation is therefore damped as it spreads through the system following its excitation. It is interesting to provide a measure of *efficiency* associated with the transport of an exciton. This can be done by requiring that a sink exists at some specific location in the system (e.g. allowing the excitation to be transferred to a neighboring equivalent system) and evaluating the probability that the exciton exits through the sink rather than decaying *non-specifically* due to recombination mechanisms.

In a master equation description, a recombination probability and a sink appear as non-Hermitian terms in the time-evolution operator for the exciton density matrix. Similarly, in our approach we ought to add damping terms to the EOM (7). More precisely, we consider a chain where the site k is identified as a sink, characterized by a trapping rate $\Gamma \gg \gamma_r$. Therefore, the modified equations of motion read

$$\mathrm{i}\hbar \frac{\mathrm{d}b_n}{\mathrm{d}t} = -\epsilon_n b_n - J_n\left(b_{n+1} + b_{n-1}\right) - \mathrm{i}\hbar\left(\gamma_r + \delta_{nk}\Gamma\right)b_n. \tag{16}$$

Along the lines of previous studies, such as [20, 82] and [83], we use equations (16) to investigate the *competition* between the two mechanisms of exciton destruction, namely generic recombination (γ_r) and exit through a specific *channel* (Γ). The whole idea is that an *efficient* transport is maximally effective in channeling the exciton rapidly through the specified exit site against the generic degradation due to recombination. For example, this might reflect an exciton leaving a light-harvesting complex through a specific pigment connected to the reaction center. Moreover, as done in the above-cited studies, we take the unperturbed exciton site energies E_n^0 in equation (16) as random, which has the well-known effect of inducing spatial localization of the exciton at zero temperature.

The incorporation of non-Hermitian terms implies a loss of norm as time passes, until eventually the norm of the exciton wave-function reaches zero for infinite times. Accordingly, a measure of transport efficiency can be computed in the following fashion

$$\eta = 2\int_0^\infty \left|b_k(t)\right|^2 \mathrm{d}t. \tag{17}$$

One can easily prove that η is finite and takes values in the interval $[0; 1]$ as a consequence of the conservation of the total excitonic amplitude when $\gamma_r = \Gamma = 0$. The integral in equation (17) can be computed numerically to any desired accuracy, as controlled by the amount of total exciton norm $N(t) = \sum_i |b_i(t)|^2$ left in the system at time t. In our simulations we integrated equations (16) until the survival probability reached the threshold value of 10^{-5}.

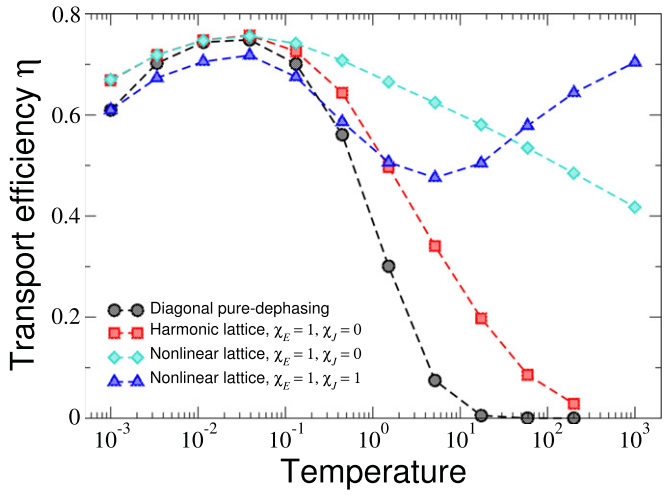

Figure 9. Exciton transport efficiency versus temperature in different kinds of lattices of length $L = 200$. The recombination constant and the sink dissipation are, respectively, $\gamma_r = 10^{-4}$ and $\Gamma = 10^{-1}$. The local unperturbed exciton energies E_n^0 are randomly chosen from a uniform distribution in the interval $[-0.5; 0.5]$. The efficiency η is obtained by averaging over 20 independent realizations of the static disorder on the site energies E_n^0 and of the dynamical lattice noise.

In figure 9 we compare the transfer efficiency of our chain model with the one corresponding to a quantum dynamics in the presence of PD noise [20, 43]. The lattice is initially thermalized at temperature T with the same procedure described in the introduction of section 3, while the PD dynamics describes the interaction of the exciton with a classical incoherent external field (no explicit lattice in this case) that induces decoherence on the quantum system. This is accomplished by specializing equations (4) and (5) to

$$\epsilon_n = E_n^0 + \sqrt{2T}\,\xi_n(t), \qquad J_n = J_n^0, \tag{18}$$

where $\xi_n(t)$ is a Gaussian white noise with zero mean and unit variance and T effectively accounts for the dephasing rate of the process. In both cases the exciton is initially injected at one side of the chain, while a trap is located at the opposite end. Interestingly, in the low-temperature region the two systems display qualitatively the same behavior, namely a disruption of disorder-induced localization due to increasing dephasing (PD model), i.e. increasing thermal fluctuations of the underlying lattice in our scheme. However, at higher temperatures the efficiency of transport in the presence of explicit (i.e. produced by the lattice) noise turns out to depend on the details of the underlying lattice dynamics. The first remarkable result is that nonlinear correlations in the lattice dynamics boost the efficiency in the Zeno-effect region (see diamonds versus squares in figure 9). This finding, although for somewhat different physical reasons, is in line with recent results where the importance of spatial correlations was demonstrated for transport in a PD-like model [83]. Furthermore, we note that such a behavior is consistent with the different scaling exponents of the diffusion constant D discussed in section 3. As a final remark, we expect that the degree of improvement with respect to the linear regime may also depend on the details of the nonlinear interaction potential for the lattice degrees of freedom.

The second important finding is that non-diagonal noise (i.e. non-zero coupling between the hopping rates in the exciton Hamiltonian and the lattice) suppresses the Zeno drop in the efficiency at high temperatures. This is in good agreement with the prediction of equation (15), namely that the diffusion coefficient should be non-monotonic with temperature (i.e. non-diagonal noise, γ_1). We recall that in this regime, the master equation for the density matrix turns into a classical diffusion equation, which should guarantee diffusive transport [48], albeit possibly with a diffusion coefficient that decreases with temperature [45].

5. Conclusions

In this paper we have studied a model describing the dynamics of a quantum excitation that propagates in a system at finite temperature. In our scheme, the quantum evolution is dictated by a TB Hamiltonian, whose matrix elements are functions of the classical coordinates of an underlying one-dimensional lattice. We refer to this setting as an open quantum system with an *explicit* environment, which provides a direct source of noise to the quantum excitation, endowed with specific spatio-temporal correlations. While the main ideas behind this modeling scheme are not new (see for example [67]), our study contains important elements of novelty. Notably, we explicitly focussed on spotlighting the signatures of non-trivial spatio-temporal correlations of nonlinear origin expressed by the underlying lattice. Furthermore, we conducted an original investigation of the relative

role of diagonal and non-diagonal exciton–phonon couplings. In both cases, we uncovered a rich phenomenology, prompting new directions of investigation.

We first examined the spreading of an initially localized excitation. Our results show that the very first stage of the propagation is faster than ballistic, up to a time of the order of $\hbar/(2J)$, J being the magnitude of the hopping integrals in the TB Hamiltonian. The subsequent time evolution is characterized by a transition to a ballistic stage followed by a crossover to an asymptotic diffusive regime, which appears at earlier and earlier times as the exciton–phonon coupling strength is increased. However, for large values of the coupling the picture changes dramatically, as a self-trapped state of nonlinear character sets in after the first super-ballistic spreading. The result is that the transport is completely suppressed in this regime as a sheer nonlinear effect.

An analysis of the diffusion coefficient D at intermediate exciton–phonon couplings unveils a striking non-monotonic behavior of D as a function of temperature, provided the lattice is actively modulating the hopping integrals in the TB Hamiltonian. This effect, reported here for the first time in the presence of an explicit environment, agrees with a long-known prediction made on the basis of a generalized master equation for the one-particle density matrix containing both dephasing and amplitude-affecting operators [43]. Intriguingly, we find that diffusive transport is faster at low temperatures with pure-diagonal noise (i.e. only on the site energies), but adding non-diagonal noise makes spreading faster at high temperatures.

Importantly, our results on the diffusive regime at intermediate coupling flag a nontrivial interconnection between exciton spreading and collective (hydrodynamic) vibrational modes of the underlying lattice. More precisely, our findings strongly suggest that the observed non-monotonic behavior of the diffusion constant versus temperature is related to the presence of long-wavelength acoustic modes. This conclusion is reinforced by a comparison with the results of Troisi and Orlandi obtained in a similar semi-classical model with purely off-diagonal dynamical disorder [45]. In fact, they found a monotonic decrease of D with temperature in a model that lacks collective vibrational modes by construction, as their TB Hamiltonian is modulated by the dynamics of an ensemble of *independent*, disconnected classical oscillators. In fact, the signatures of long-wavelength hydrodynamic modes are clearly recognizable in the equilibrium power spectra $S(k, \omega)$ of the exciton-coupled lattice, as shown in figure 1. This strongly suggests that coupling to an *extended* dynamical system, such as the one we consider here, might be a necessary condition to obtain non-monotonic transport with temperature, in agreement with [43].

Our results on the role of the lattice in the spreading properties of a quantum excitation show that the presence of non-diagonal coupling is sufficient to suppress Zeno-like localization at high temperature. To shed further light into this phenomenon, we then computed a measure of quantum efficiency for different choices of the chain parameters. Our results clearly confirm that, when the hopping rates in the TB Hamiltonian are explicitly modulated by the lattice dynamics, the transport efficiency is no longer quenched at high temperature, as observed by some authors in the absence of an *explicit* environment [19, 20]. Moreover, we find that nonlinearity in the lattice dynamics exerts a powerful boosting action on the efficiency at high temperatures, confirming recent results on the importance of spatial and dynamical correlation patterns within the noise bath [83].

Overall, the results presented in this paper allow us to conclude that the properties of excitonic systems interacting with noisy environments are subtly shaped by the specific properties of the exciton–phonon coupling and by the nature of the spatio-temporal dynamical correlations that characterize the underlying lattice. It would be extremely interesting to extend the formalism presented here to more complex systems, such as light-harvesting complexes, which are widely studied in the context of quantum biology [85, 84].

Acknowledgments

The authors acknowledge financial support from the EU FP7 project PAPETS (GA 323901). YO and OB thank the support from Fundação para a Ciência e a Tecnologia (Portugal), namely through programmes PTDC/POPH and projects PEst-OE/EGE/UI0491/2013, PEst-OE/EEI/LA0008/2013, UID/EEA/50008/2013, IT/QuSim and CRUP-CPU/CQVibes, partially funded by EU FEDER and from the EU FP7 project LANDAUER (GA 318287).

References

[1] Law M, Goldberger J and Yang P 2004 *Annu. Rev. Mater. Res.* **34** 83–122
[2] Yanson A I, Bolainger G R, van den Brom H E, Agrait N and van Ruitenbeek J M 1998 *Nature* **395** 783–5
[3] Roati G, D'Errico C, Fallani L, Fattori M, Fort C, Zaccanti M, Modugno G, Modugno M and Inguscio M 2008 *Nature* **453** 895–8
[4] Perebeinos V, Tersoff J and Avouris P 2004 *Phys. Rev. Lett.* **92** 257402
[5] Wang F, Cho D J, Kessler B, Deslippe J, Schuck P J, Louie S G, Zettl A, Heinz T F and Shen Y R 2007 *Phys. Rev. Lett.* **99** 227401
[6] Zhao H, Mazumdar S, Sheng C X, Tong M and Vardeny Z V 2006 *Phys. Rev.* B **73** 075403

[7] Lee J, Hernandez P, Lee J, Govorov A O and Kotov N A 2007 *Nat. Mater.* **6** 291–5
[8] Scholes G D and Rumbles G 2006 *Nat. Mater.* **5** 683–96
[9] Blankenship R E 2002 *Molecular Mechanisms of Photosynthesis* (Oxford: Blackwell Science)
[10] van Amerongen H, Valkunas L and van Grondelle R 2000 *Photosynthetic Excitons* (Singapore: World Scientific)
[11] Frenkel J 1931 *Phys. Rev.* **37** 17–44
[12] Davydov A S 1948 *Zh. Eksp. Teor. Fiz.* **18** 210–8
[13] Engel G S, Calhoun T R, Read E L, Ahn T K, Mancal T, Cheng Y C, Blankenship R E and Fleming G R 2007 *Nature* **446** 782–6
[14] Read E L, Lee H and Fleming G R 2009 *Photosynth. Res.* **101** 233–43
[15] Collini E, Wong C Y, Wilk K E, Curmi P M G, Brumer P and Scholes G D 2010 *Nature* **463** 644–7
[16] Romero E, Augulis R, Novoderezhkin V I, Ferretti M, Thieme J, Zigmantas D and van Grondelle R 2014 *Nat. Phys.* **10** 676–82
[17] Collini E and Scholes G D 2009 *Science* **323** 369–73
[18] Chin A W, Prior J, Rosenbach R, Caycedo-Soler F, Huelga S F and Plenio M B 2013 *Nat. Phys.* **9** 113–8
[19] Chin A W, Datta A, Caruso F, Huelga S F and Plenio M B 2010 *New J. Phys.* **12** 065002
[20] Rebentrost P, Mohseni M, Kassal I, Lloyd S and Aspuru-Guzik A 2009 *New J. Phys.* **11** 033003
[21] O'Reilly E J and Olaya-Castro A 2014 *Nat. Commun.* **5** 3012
[22] Tiwari V, Peters W K and Jonas D M 2013 *Proc. Natl Acad. Sci. USA* **110** 1203–8
[23] Mennucci B and Curutchet C 2011 *Phys. Chem. Chem. Phys.: PCCP* **13** 11538–50
[24] Plenio M B and Huelga S F 2008 *New J. Phys.* **10** 113019
[25] Skourtis S S and Beratan D N 2007 *Science* **316** 703–4
[26] Lee H, Cheng Y C and Fleming G R 2007 *Science* **316** 1462–5
[27] Wang H, Lin S, Allen J P, Williams J C, Blankert S, Laser C and Woodbury N W 2007 *Science* **316** 747–50
[28] Adolphs J and Renger T 2006 *Biophys. J.* **91** 2778–97
[29] Saito K and Dhar A 2007 *Phys. Rev. Lett.* **99** 180601
[30] Chetverikov A P, Ebeling W and Velarde M G 2009 *Eur. Phys. J.* B **70** 217–27
[31] Komarnicki S and Hennig D 2003 *J. Phys.: Condens. Matter* **15** 441
[32] Leitner D M 2001 *Phys. Rev.* B **64** 094201
[33] Platero G and Aguado R 2004 *Phys. Rep.* **395** 1–57
[34] Mulansky M and Pikovsky A 2013 *New J. Phys.* **15** 053015
[35] Ivanchenko M V, Laptyeva T V and Flach S 2011 *Phys. Rev. Lett.* **107** 240602
[36] Flach S 2010 *Chem. Phys.* **375** 548–56
[37] García-Mata I and Shepelyansky D L 2009 *Phys. Rev.* E **79** 026205
[38] Kopidakis G, Komineas S, Flach S and Aubry S 2008 *Phys. Rev. Lett.* **100** 084103
[39] Vlaming S M and Silbey R J 2012 *J. Chem. Phys.* **136** 055102
[40] Chen X and Silbey R J 2010 *J. Chem. Phys.* **132** 204503
[41] Aragó J and Troisi A 2015 *Phys. Rev. Lett.* **114** 026402
[42] Troisi A 2011 *Chem. Soc. Rev.* **40** 2347–58
[43] Schwarzer E and Haken H 1972 *Phys. Lett.* A **42** 317–8
[44] Haken H and Strobl G 1973 *Z. Phys.* **262** 135–48
[45] Troisi A and Orlandi G 2006 *Phys. Rev. Lett.* **96** 086601
[46] Breuer H P and Petruccione F 2002 *The Theory of Open Quantum Systems* (Oxford: Oxford University Press)
[47] Rivas A and Huelga S F 2012 *Open Quantum Systems: An Introduction* (Berlin: Springer)
[48] Schwarzer E and Haken H 1972 *Phys. Lett.* A **42** 317–8
[49] Lindblad G 1976 *Commun. Math. Phys.* **48** 119
[50] Gorini V, Kossakowski A and Sudarshan E C G 1976 *J. Math. Phys.* **17** 821
[51] Nakajima S 1958 *Prog. Theor. Phys.* **20** 948–59
[52] Ishizaki A and Fleming G R 2009 *Proc. Natl Acad. Sci.* **106** 17255–60
[53] Chen X and Silbey R J 2011 *J. Phys. Chem.* B **115** 5499–509
[54] Prior J, Chin A W, Huelga S F and Plenio M B 2010 *Phys. Rev. Lett.* **105** 050404
[55] Boninsegna L and Faccioli P 2012 *J. Chem. Phys.* **136** 214111
[56] Huo P and Coker D F 2010 *J. Chem. Phys.* **133** 133
[57] Makri N and Makarov D E 1995 *J. Chem. Phys.* **102** 4600–10
[58] Kurnosov A A, Rubtsov I V and Burin A L 2015 *J. Chem. Phys.* **142** 011101
[59] Shim S, Rebentrost P, Valleau S and Aspuru-Guzik A 2012 *Biophys. J.* **102** 649–60
[60] Gutiérrez R, Caetano R A, Woiczikowski B P, Kubar T, Elstner M and Cuniberti G 2009 *Phys. Rev. Lett.* **102** 208102
[61] Cheung D L, McMahon D P and Troisi A 2009 *J. Phys. Chem.* B **113** 9393–401
[62] Viani L, Corbella M, Curutchet C, O'Reilly E J, Olaya-Castro A and Mennucci B 2014 *Phys. Chem. Chem. Phys.* **16** 16302–11
[63] Hennig D 2001 *Eur. Phys. J.* B **381** 377–81
[64] Mingaleev S F, Christiansen P L, Gaididei Y B, Johansson M and Rasmussen K O 1999 *J. Biol. Phys.* **25** 41–63
[65] Bittner E R, Goj A M and Burghardt I 2010 *Chem. Phys.* **370** 137–42
[66] Freedman H, Martel P and Cruzeiro L 2010 *Phys. Rev.* B **82** 174308
[67] Davydov A S 1962 *Theory of Molecular Excitons* (New York: McGraw-Hill)
[68] Scott A 1992 *Phys. Rep.* **217** 1–67
[69] Holstein T 1959 *Ann. Phys., NY* **8** 325–42
[70] Kalosakas G, Aubry S and Tsironis G P 1998 *Phys. Rev.* B **58** 3094–104
[71] Su W P, Schrieffer J R and Heeger A J 1979 *Phys. Rev. Lett.* **42** 1698–701
[72] Fermi E, Pasta J and Ulam S 1955 *Los Alamos Rep.* LA 1940
[73] Butt I A and Wattis J A 2007 *Physica* D **231** 165–79
[74] Lepri S, Livi R and Politi A 2003 *Phys. Rep.* **377** 1
[75] Fleischer J W, Segev M, Efremidis N K and Christodoulides D N 2003 *Nature* **422** 147–50
[76] Franzosi R, Livi R, Oppo G L and Politi A 2011 *Nonlinearity* **24** R89
[77] Flach S and Gorbach A V 2008 *Phys. Rep.* **467** 1–116
[78] Trombettoni A and Smerzi A 2001 *Phys. Rev. Lett.* **86** 2353–6
[79] Davydov A S 1979 *Phys. Scr.* **20** 387

[80] Cruzeiro-Hansson L and Kenkre V 1995 *Phys. Lett.* A **203** 362–6
[81] Misra B and Sudarshan E C G 1977 *J. Math. Phys.* **18** 756–63
[82] Novo L, Mohseni M and Omar Y 2013 arXiv:1312.6989
[83] Pelzer K M, Fidler A F, Griffin G B, Gray S K and Engel G S 2013 *New J. Phys.* **15** 095019
[84] Mohseni M, Omar Y, Engel G and Plenio M B (ed) 2014 *Quantum Effects in Biology* (Cambridge: Cambridge University Press)
[85] Huelga S F and Plenio M B 2013 *Contemp. Phys.* **54** 181–207